Exciton scattering and localization in branched dendrimeric structures

CHAO WU[1], SERGEY V. MALININ[1], SERGEI TRETIAK[2]* AND VLADIMIR Y. CHERNYAK[1]*

[1]Department of Chemistry, Wayne State University, 5101 Cass Ave, Detroit, Michigan 48202, USA

[2]Theoretical Division, Center for Nonlinear Studies, and Center for Integrated Nanotechnologies, Los Alamos National Laboratory, Los Alamos, New Mexico 87545, USA

*e-mail: serg@lanl.gov; chernyak@chem.wayne.edu

Published online: 27 August 2006; doi:10.1038/nphys389

π-conjugated dendrimers are molecular examples of tree-like structures known in physics as Bethe lattices. Electronic excitations in these systems can be spatially delocalized or localized depending on the branching topology. Without *a priori* knowledge of the localization pattern, understanding photoexcitation dynamics reflected in experimental optical spectra is difficult. 'Supramolecular'-like quantum-chemical calculations quickly become intractable as the molecular size increases. Here we develop a reduced exciton-scattering (ES) model, which attributes excited states to standing waves in quasi-one-dimensional structures, assuming a quasiparticle picture of optical excitations. Direct quantum-chemical calculations of branched phenylacetylene chromophores are used to verify our model and to derive relevant parameters. Complex and non-trivial delocalization patterns of photoexcitations throughout the entire molecular tree can then be universally characterized and understood using the proposed ES method, completely bypassing 'supramolecular' calculations. This allows accurate modelling of excited-state dynamics in arbitrary branched structures.

Conjugated polymers and molecular wires are promising materials for a number of technological applications, such as light-emitting, lasing and molecular electronics applications[1,2]. Their extended one-dimensional backbones support delocalized mobile π-electron systems. This results in a semiconductor-like electronic structure, which may be manipulated synthetically. Branching of linear chains produces tree-like molecules (dendrimers) that can be used to extend desirable electronic properties even further[3,4]. In particular, dendrimers are believed to be promising building blocks for artificial light-harvesting systems[5–8]. These considerations are based on their unique geometric structures known as Cayley trees or Bethe lattices: as the dendrimer progresses to a higher generation, the exponentially increasing peripheral terminal chromophores serve as an antenna matrix to gather the incoming light. The collected energy in the form of photogenerated electronic excitations is further funnelled to the core, where it can trigger chemical reactions. Cooperative enhancement of nonlinear optical responses (such as two-photon absorption) in dendrimers is another currently active field of research[9,10].

Studies investigating artificial light-harvesting functionality in dendrimeric structures revealed a fascinating interplay between photoexcitation localization/delocalization patterns and their energy-relaxation dynamics. In contrast to fluorescence resonance energy transfer from peripheral dyes directly to the core dye, observed in flexible polyarylether backboned dendrimers[5], fully conjugated symmetrical globular phenylacetylene dendrimers[7,11] transfer excitations sequentially through the conjugated net[12]. In the latter structures, linear oligomers form rigid monodendrons linked via meta-substituted phenyl rings. Meta-substitutions break the conjugation leading to efficient localization of photogenerated excitations in the linear segments[7,13–17]. The energy gradient is then automatically created as the core extends to higher generations with shorter phenylacetylene segments. The delicate interplay of strong and weak coupling between linear chromophores has specific signatures in the temperature-dependent dynamics and vibrational system relaxation[16–18]. The ortho-substitution linkage is less favourable relative to the meta one due to steric interactions. However, several unsymmetrical dendrimers with few generations were recently synthesized by Peng and co-workers[8,19,20]. These use both ortho- and para-substituted phenyls as joints to connect the phenylacetylene segments. As the optical and

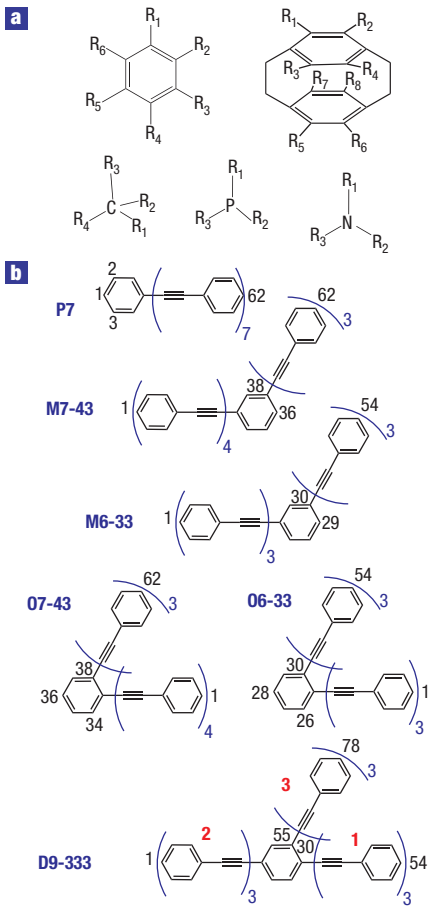

Figure 1 Supramolecular dendrimers are made up via branching of linear chains. a, Examples of branching centres. **b**, Structure and atom labelling of the 'para' P7, 'meta' M6-33 and M7-43, 'ortho' O6-33 and O7-43 and branched D9-333 molecules considered in this article.

photophysical properties of these systems are significantly different from those of symmetrical branching structures, the fundamental photoexcitation dynamics in unsymmetrical dendrimers could be different, and the energy-transfer mechanisms are not well understood[19,20]. Moreover, photoprocesses in compounds using alternatives to phenyl-based branching centres (for example, nitrogen or phosphorus)[9,10] have not been explored in detail, and the universal theoretical understanding encompassing all branching structures (several examples are shown in Fig. 1a) is yet to be determined.

EXCITON-SCATTERING MODEL

We propose the exciton-scattering (ES) model to allow clear interpretation of photoexcitation delocalization in arbitrary branched structures. Excitons in infinitely long linear conjugated chains can be treated as quasiparticles with well-defined momenta. Excited states in finite systems have pronounced node structure and can be related to the excitations with non-zero momenta[21]. For linear molecules, this correspondence was explored in the context of electron-energy-loss spectroscopy[22,23]. The ES approach extends these developments to a more general case and naturally attributes excited states in branched structures to standing waves that result from exciton scattering at the molecular ends, joints and branching vertices. The ES model rests on the assumption of decoupling between the centre-of-mass and relative motion of electron–hole pairs and is asymptotically exact in the limit of the exciton size being short compared with the linear segment lengths. Any branched organic molecule is then treated as a graph[24]. The excited states are represented by wavefunctions $\psi_s(x) = a_s \exp(ikx_s) + b_s \exp(-ikx_s)$ of the exciton centre-of-mass position x_s on the segments. These two plane waves describe the quantum quasiparticle motion in two possible directions in a linear segment. The wavevectors are related to the exciton frequencies through the exciton spectrum $\omega(k)$ in the infinite-length chains. In a vertex that connects n linear segments, the amplitudes of the outgoing plane waves are related to the incoming waves' amplitudes through an $n \times n$ scattering matrix[25] $\Gamma^{(n)}_{rs}(\omega)$. Naturally, the off-diagonal and diagonal elements of Γ describe transmission and reflection processes, respectively. The Frenkel exciton model seems to be the limiting case in this approach, allowing only for complete reflection or transmission. Exciton frequencies and wavefunctions can be found by solving a simple linear problem for the amplitudes a_s and b_s. For a molecule represented by a graph with d_1 edges (linear segments) we have $2d_1$ independent variables (amplitudes). At each vertex/branching a of degree n_a, we have n_a linear equations that connect the amplitudes of the outgoing waves in terms of their incoming counterparts through the elements of the scattering matrix $\Gamma^{(n_a)}_a$. The number of linear equations $\sum_a n_a = 2d_1$ exactly matches the number of variables, and we arrive at a linear homogeneous $2d_1 \times 2d_1$ frequency-dependent problem. The solution gives the transition frequencies of the excited states and the shapes of the standing waves, containing all information on the electronic spectrum of a macromolecule.

This provides a dramatic reduction in the computational effort compared with 'supramolecular'-like quantum-chemical approaches and allows swift evaluation of novel organic materials for desirable electronic properties. On the other hand, the ES model builds on the high-quality electronic-structure calculations, such as time-dependent density functional theory[26], by requesting the electronic-structure data on linear segments and relevant vertices as an input. This can be done routinely using standard quantum-chemical codes and very modest computational resources. The chosen level of quantum chemistry can be rather arbitrary, however, it should be capable of describing excitonic effects in the excited states. Excitons are vitally important for the description of excited-state structure and photoinduced dynamics in conjugated chromophores. These quasiparticles are fundamental objects in the ES approach. Approaches on the basis of the local (or non-hybrid general gradient) density approximations, Hartree–Fock, or simpler tight-binding (Hückel) models do not reproduce photoexcited bound states of electrons and holes[27], and, thus, should not be used in conjunction with our model.

RESULTS OF QUANTUM-CHEMICAL CALCULATIONS

To illustrate practical applications of the ES theoretical framework, we consider several phenylacetylene oligomers branching at para-, ortho- and meta-positions at substituted phenyl rings, as shown in Fig. 1b. Similar compounds have recently been explored experimentally[28]. The excited-state structure of these molecules was calculated quantum-chemically as described in the Methods section. The computed states are strongly delocalized π–π excitations, which are optically accessible and play a crucial role in energy-transfer processes. Typically, the lowest-energy (bandgap) transition in such conjugated linear chains has remarkable oscillator strength and characteristically appears as a main peak in the linear absorption spectra[29,30]. Figure 2 summarizes our main computational results. The contour plots represent the transition density matrices $(\xi_\nu)_{mn}$ (also referred to as electronic normal

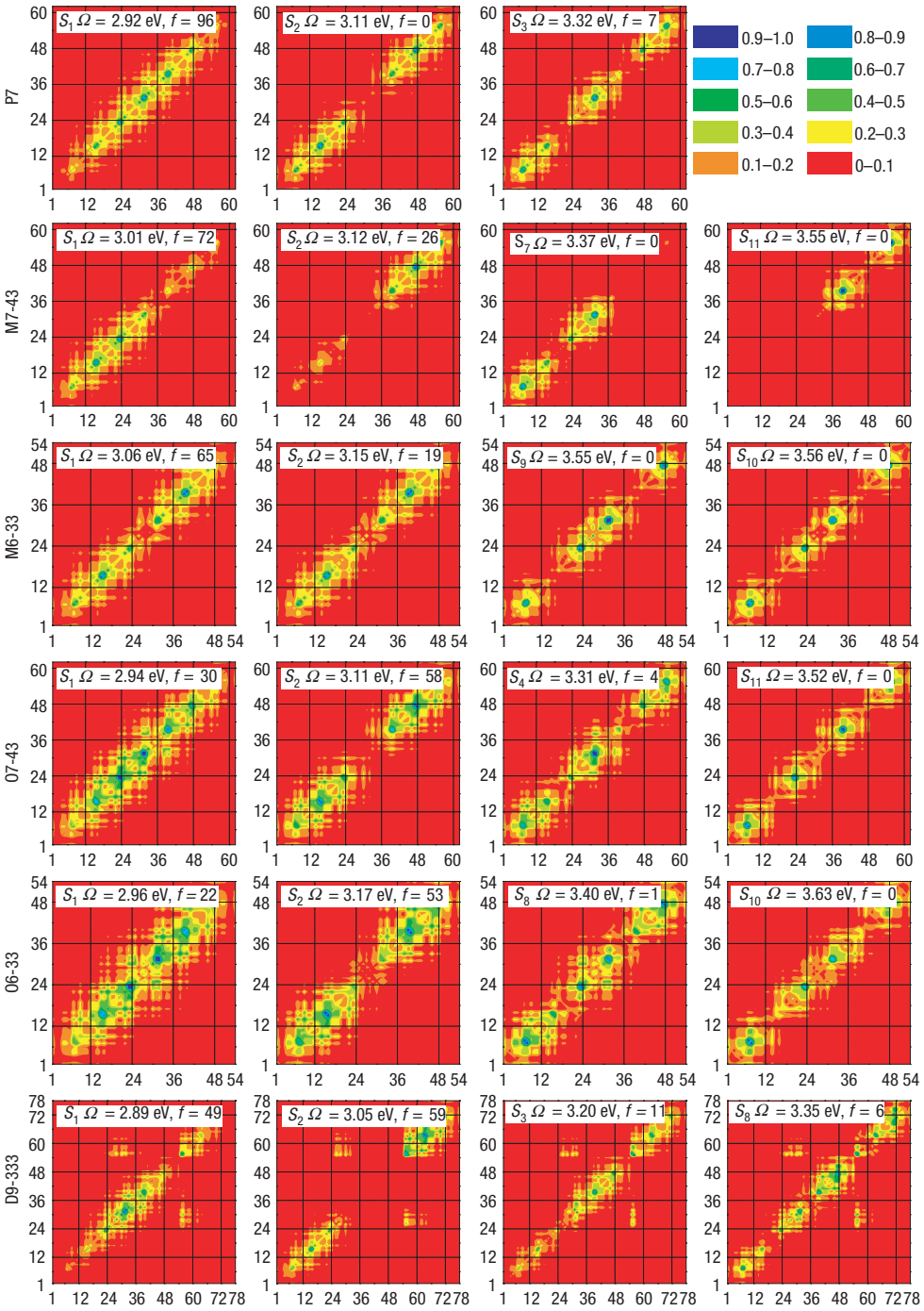

Figure 2 Exciton-scattering patterns given by contour plots of transition density matrices from the ground state to excited states of the molecules shown in Fig. 1. Each plot shows the probability amplitudes of an electron moving from one molecular position (horizontal axis) to another (vertical axis) on electronic excitation. The axis labels represent individual carbon atoms according to the labelling in Fig. 1. The inset in each plot shows the excited state number (for example, S_{11} is the eleventh singlet state), its transition frequency Ω and oscillator strength f.

modes) between the ground and electronically excited states, as 'topographic' maps that reflect the single-electron reduced density matrix changes on molecular photoexcitation[29,31].

To establish a reference point, we start with the linear chain P7. The results are shown in the first row. S_1 represents the bandgap transition and can be associated with $k = 0$ momentum exciton in the infinite chain limit. The electron–hole pair created on optical excitation is delocalized over the entire chain (diagonal in the plot). The exciton size (maximal distance between electron and hole) is about 3 repeat units (largest off-diagonal extent of the non-zero matrix area). The higher-frequency electronic transitions (S_2, S_3 and so on) have characteristic node structure and correspond to the excitons with non-zero momenta.

The second row in Fig. 2 shows excited states of M7-43. The meta-connection clearly breaks the molecule into two linear segments. The excited states of the molecule, S_1 and S_2 (S_7 and S_{11}),

directly correspond to S_1 (S_2) excitation of the linear oligomers P4 and P3, respectively. An electrostatic coupling between S_1 and S_2 of M7-43 can be related to the interaction of transition dipoles of S_1 states of P4 and P3. This leads to shifts in the electronic energy levels, and slightly mixes S_1 states of P4 and P3. Owing to vanishing oscillator strengths, this mixing becomes weaker for higher-lying states S_7 and S_{11}. A very similar situation is observed in the second meta-compound M6-33, with the exception that the excitation energies of its linear segments P3 are the same. Subsequently, the lowest excited states S_1 and S_2 are coherent 'plus' and 'minus' superpositions of the S_1 (P3) excitations. These are Frenkel-type excitons[15,32], characteristic for molecular aggregates. The splitting between S_1 and S_2 states of M6-33 measures the coupling strength. Both S_1 and S_2 states have non-zero oscillator strengths resulting as a vector sum of the corresponding transition dipoles. Thus, meta-based connections effectively break the branching structure into a number of electrostatically interacting chromophores, which makes it possible to apply reduced Frenkel-like hamiltonian models[15,32].

Next, we analyse the properties of ortho-branching. The lowest state S_1 in both O7-43 and O6-33 looks very similar to the S_1 state of the linear chromophore P7. The higher-lying excited states of O7-43 and O6-33 also have characteristic node structures, irrespective of the position of the ortho-joint along the chain (compare the fourth and fifth rows with the first row in Fig. 2). This clearly demonstrates that ortho-branching does not prevent exciton delocalization and the excitation pattern is similar to that in the linear chains. However, there are important differences between para- and ortho-connections. The second excited state S_2 in both O7-43 and O6-33 appears as the state with the largest oscillator strength in their spectra, whereas it is optically forbidden in the linear chromophore P7. At the same time, the bandgap state S_1 of O7-43 and O6-33 has a relatively small oscillator strength compared with that of P7. This redistribution of the oscillator strength among excitons in the band is a manifestation of molecular geometry. Compared with the linear chains, where both parts contribute nearly evenly to the total oscillator strength of the S_1 state, the transition dipole of the S_1 state in the ortho-structures is reduced due to vector addition of the dipole components on the linear segments. Albeit the S_2 state gains strong oscillator strength for the same reason. Subsequently, states that are optically forbidden in the linear chains, can be experimentally detected in the ortho-structures, whose linear absorptions are expected to have several low-lying peaks. In contrast to meta-compounds, which have independent interacting linear chromophores, these states in ortho-molecules appear due to transfer of the oscillator strength to the high-lying excitons as a consequence of molecular geometry.

After the methodological study of possible phenyl-based joints, we consider a combined structure D9-333 (Fig. 1b). The bottom row of Fig. 2 shows transition density matrices of the optically relevant excited states. Unlike previous cases, their interpretation using the delocalization/localization language[14,15] does not look straightforward. For example, ortho-branching assumes fully delocalized states, whereas S_2 shows clear localization trends.

APPLICATION OF EXCITON-SCATTERING MODEL

The ES approach allows a uniform interpretation of all molecular examples considered (Fig. 1b). The ES system of linear equations adopts the form:

$$b_s \exp(-ikl_s) = \Gamma^{(1)}(\omega) a_s \exp(ikl_s); \quad a_s = \sum_r \Gamma^{(n)}_{sr}(\omega) b_r.$$

where l_s are the linear segment lengths; $n = 2$ for M and O molecules and $n = 3$ for the D branched structure. In the latter case $r, s = 1, 2, 3$ correspond to the right, left and upper linear segments, respectively. A qualitatively correct zero-order approximation for the scattering matrix Γ can be readily constructed. The molecular end is a vertex with $n = 1$. Vanishing of the excitonic wavefunction at the ends implies full reflection $\Gamma^{(1)} = -1$. The central vertex of M molecules is described by a 2×2 scattering matrix $\Gamma^{(\mathrm{meta})}_{12} = \Gamma^{(\mathrm{meta})}_{21} = 0$, $\Gamma^{(\mathrm{meta})}_{11} = \Gamma^{(\mathrm{meta})}_{22} = -1$, which accounts for the full reflection at meta-connection. The full transmission of ortho-vertex in O compounds implies: $\Gamma^{(\mathrm{ortho})}_{12} = \Gamma^{(\mathrm{ortho})}_{21} = 1$, $\Gamma^{(\mathrm{ortho})}_{11} = \Gamma^{(\mathrm{ortho})}_{22} = 0$. This assignment immediately rationalizes similarity in the shapes and energies between the S_2 (M6-33) and S_2 (O6-33), or S_{10} (M6-33) and S_{10} (O6-33) states (see Fig. 2): they have the same excitonic wavefunction. The small differences can be attributed to deviations in the scattering matrices from the zero-order approximation due to, for example, steric interactions.

We further illustrate our ES model for the D9-333 molecule. The analogous rationale can be applied to derive the scattering matrix for an arbitrary branching centre. Similar properties of para- and ortho-joints (to the zero-order approximation) imply symmetry of the scattering matrix $\Gamma^{(3)}_{rs}$ with respect to interchange of branches 2 (left) and 3 (upper) of D9-333 (red labels in Fig. 1b), that is, $\Gamma^{(3)}_{22} = \Gamma^{(3)}_{33}$, $\Gamma^{(3)}_{23} = \Gamma^{(3)}_{32}$, $\Gamma^{(3)}_{12} = \Gamma^{(3)}_{13}$ and $\Gamma^{(3)}_{21} = \Gamma^{(3)}_{31}$. This leaves us with five independent components of the scattering matrix: $\Gamma^{(3)}_{11}$, $\Gamma^{(3)}_{22}$, $\Gamma^{(3)}_{23}$, $\Gamma^{(3)}_{12}$ and $\Gamma^{(3)}_{21}$. Excitonic wavefunctions can be classified by their parity with respect to interchange of branches 2 and 3. Odd exciton modes vanish on branch 1, they are fully characterized by the amplitudes a_2 and b_2 that can be found by solving a linear problem in an effective linear chain that represents branch 2. The scattering amplitudes at the left and right ends are $\Gamma^{(1)} = -1$ and $\Gamma^{(-)} = \Gamma^{(3)}_{22} - \Gamma^{(3)}_{23}$, respectively. Even exciton modes are characterized by the amplitudes a_s and b_s with $s = 1, 2$. They can be found by solving a linear problem in an effective linear chain that represents branches 1 and 2 with a joint in the centre. The joint is described by an effective 2×2 scattering matrix with the elements $\Gamma^{(+)}_{21} = \sqrt{2}\Gamma^{(3)}_{21}$, $\Gamma^{(+)}_{12} = \sqrt{2}\Gamma^{(3)}_{12}$, $\Gamma^{(+)}_{22} = \Gamma^{(3)}_{22} + \Gamma^{(3)}_{23}$ and $\Gamma^{(+)}_{11} = \Gamma^{(3)}_{11}$. The para–ortho-joints symmetry is confirmed by vanishing of the S_2 mode in D9-333 on the right branch and its striking similarity to the S_1 mode in M6-33 in terms of shape, energy and oscillator strength. The similarity in the energy and oscillator strength means that the modes have similar wavefunctions, which implies $\Gamma^{(-)} = \Gamma^{(3)}_{22} - \Gamma^{(3)}_{23} = -1$. The even modes S_1, S_3 and S_8 of D9-333 have 0, 1 and 2 nodes in the effective linear molecule, as clearly seen from Fig. 2. They are similar in terms of the shapes and energies to the S_1, S_2 and S_8 modes, respectively, of the O6-33 molecule. This implies for the zero-order approximation $\Gamma^{(+)}_{11} = \Gamma^{(+)}_{22} = 0$ and $\Gamma^{(+)}_{12} = \Gamma^{(+)}_{21} = 1$. Finally, we arrive at $\Gamma^{(3)}_{11} \approx 0$, $\Gamma^{(3)}_{12} \approx \Gamma^{(3)}_{21} \approx 1/\sqrt{2}$, $\Gamma^{(3)}_{22} \approx -1/2$ and $\Gamma^{(3)}_{23} \approx 1/2$, which completes the scattering matrix form. The differences in the corresponding energies and irregularities in the node positions in D9-333 are attributed to the deviation of the scattering matrix $\Gamma^{(3)}_{rs}$ from its simple zero-order approximation, which turns out to be small. Strong differences in the oscillator strengths are due to different geometries of these molecules.

In conclusion, we establish stable and intuitively clear relationships between the structure of optical excitations in branched organic molecules and the underlying molecular geometry. The excitation localization/delocalization concept of molecular aggregates, previously successfully used for meta-conjugated dendrimers[7,14–16], fails in the case of general branched structures, which involve various combinations of joints and branching[5,9,17]. The proposed ES model provides simple, yet quantitatively correct, microscopic insight into electronic spectra in such quasi-one-dimensional organic structures with complex topology[3–5]. It is conceptually reminiscent of the graph theory[24] and the Hückel model applications[33,34] to chemical reactivity. The ES approach is based on very common-life concepts, such as wave

propagation, scattering and reflection, as well as the formation of standing waves, nodes and so on. This allows simple and clear visualization of non-trivial and often counterintuitive quantum-mechanical phenomena involved in the electronic structure of complex nanosized molecules. The ES picture is confirmed by direct quantum-chemical calculations, which show pronounced node structure of electronic modes, full reflection from meta-joints and almost full transmission through ortho-connections, even for relatively short linear segments. Well-recognizable interference patterns reflect the non-trivial structure of exciton scattering at branching vertices, which, in principle, could contain all possible options, that is, a reflected as well as two or more transmitted waves. The reported results contain a number of predictions that can be verified experimentally, for example, spectroscopic signatures of excitons with non-zero momenta in ortho-compounds appearing due to molecular geometry. Even although we only consider the phenyl-centred branching case here, our approach is applicable to any structure with arbitrary branching centres[9,17]. We also note that the semi-empirical collective electronic oscillator technique[29,31] used in this study on a proving-the-concept basis is a matter of convenience, rather than necessity. The scattering model can be easily coupled to any first-principle approach, where quantum-chemical calculations of branching vertices and linear segments will provide a more accurate approximation for the scattering matrices. This ensures a quantitatively correct description of complex electronic phenomena and overcomes many fundamental limitations (restricted parameterization or lack of many-body effects) of the previous reduced models, for example, the Hückel or Frenkel exciton model, while preserving their conceptual simplicity. Thus, the ES concept is an attractive approach to gain fundamental understanding of the excited-state electronic structure in complex branched molecules of general connectivity, and is likely to provide an efficient microscopic insight for design and engineering of organic molecules with desired optical and photophysical properties.

METHODS

We conducted quantum-chemical calculations of several model phenylacetylene oligomers in Fig. 1b. For the linear oligomer P7, the symbol P denotes para and 7 stands for seven repeat units. The M6-33 (M7-43) compound represents a linkage of two oligomers of three and three (four and three) phenylacetylene repeat units at a meta-position. Similarly, O6-33 and O7-43 exemplify possible ortho-connections of two linear segments. Finally, D9-333 is a combination of para-, meta- and ortho-linkages with three arms, which is a branching segment of an unsymmetrical dendrimer.

The ground-state geometries of all molecules (Fig. 1b) were optimized using the Gaussian 03[35] package at the AM1 semi-empirical level. The geometry optimization resulted in planar molecular structures. Some conformational disorder is expected in real materials due to solvent and temperature effects[7,13–17]. Several lowest optically relevant excited states were then calculated using the time-dependent Hartree–Fock approximation in combination with the intermediate neglect of differential overlap/spectroscopy (INDO/S) hamiltonian as implemented in the collective electronic oscillator code[30,31]. This approach worked quite accurately in the past for similar chromophores[14,29,31].

These calculations characterize each excited state via the vertical excitation energy, optical oscillator strength and electronic transition density matrix (or electronic normal mode). The latter bears important information on the changes in the molecular density and coherences induced on optical excitation. This can be visualized using a two-dimensional real-space representation (Fig. 2). Within the time-dependent Hartree–Fock approach, the diagonal elements $(\xi_\nu)_{nn}$ of the matrices describe the net charge induced in the nth atom by the external field. The off-diagonal elements $(\xi_\nu)_{mn}$ with $m \neq n$ represent the joint probability amplitude of finding an electron and a hole located at the mth and nth atoms, respectively[31]. Thus, the transition density matrices show the spatial extent of electronic transitions with optically induced charges and electronic coherences.

Received 22 March 2006; accepted 28 July 2006; published 27 August 2006.

References

1. Friend, R. H. *et al.* Electroluminescence in conjugated polymers. *Nature* **397,** 121–128 (1999).
2. Forrest, S. R. The path to ubiquitous and low-cost organic electronic appliances on plastic. *Nature* **428,** 911–918 (2004).
3. Percec, V. *et al.* Self-organization of supramolecular helical dendrimers into complex electronic materials. *Nature* **419,** 384–387 (2002).
4. Yaliraki, S. N. & Ratner, M. A. Interplay of topology and chemical stability on the electronic transport of molecular junctions. *Ann. NY Acad. Sci.* **960,** 153–162 (2002).
5. Gilat, S. L., Adronov, A. & Frechet, J. M. J. Light harvesting and energy transfer in novel convergently constructed dendrimers. *Angew. Chem. Int. Edn* **38,** 1422–1427 (1999).
6. Gust, D., Moore, T. A. & Moore, A. L. Mimicking photosynthetic solar energy transduction. *Acc. Chem. Res.* **34,** 40–48 (2001).
7. Kopelman, R. *et al.* Spectroscopic evidence for excitonic localization in fractal antenna supermolecules. *Phys. Rev. Lett.* **78,** 1239–1242 (1997).
8. Peng, Z. H., Pan, Y. C., Xu, B. B. & Zhang, J. H. Synthesis and optical properties of novel unsymmetrical conjugated dendrimers. *J. Am. Chem. Soc.* **122,** 6619–6623 (2000).
9. Goodson, T. G. Optical excitations in organic dendrimers investigated by time-resolved and nonlinear optical spectroscopy. *Acc. Chem. Res.* **38,** 99–107 (2005).
10. Goodson, T. G. Time-resolved spectroscopy of organic dendrimers and branched chromophores. *Ann. Rev. Phys. Chem.* **56,** 581–603 (2005).
11. Devadoss, C., Bharathi, P. & Moore, J. S. Energy transfer in dendritic macromolecules: Molecular size effects and the role of an energy gradient. *J. Am. Chem. Soc.* **118,** 9635–9644 (1996).
12. Heijs, D. J., Malyshev, V. A. & Knoester, J. Trapping time statistics and efficiency of transport of optical excitations in dendrimers. *J. Chem. Phys.* **121,** 4884–4892 (2004).
13. BarHaim, A., Klafter, J. & Kopelman, R. Dendrimers as controlled artificial energy antennae. *J. Am. Chem. Soc.* **119,** 6197–6198 (1997).
14. Tretiak, S., Chernyak, V. & Mukamel, S. Localized electronic excitations in phenylacetylene dendrimers. *J. Phys. Chem. B* **102,** 3310–3315 (1998).
15. Poliakov, E. Y., Chernyak, V., Tretiak, S. & Mukamel, S. Exciton-scaling and optical excitations of self-similar phenylacetylene dendrimers. *J. Chem. Phys.* **110,** 8161–8175 (1999).
16. Thompson, A. L., Gaab, K. M., Xu, J. J., Bardeen, C. J. & Martinez, T. J. Variable electronic coupling in phenylacetylene dendrimers: The role of Forster, Dexter, and charge-transfer interactions. *J. Phys. Chem. A* **108,** 671–682 (2004).
17. Ortiz, W., Krueger, B. P., Kleiman, V. D., Krause, J. L. & Roitberg, A. E. Energy transfer in the nanostar: The role of coulombic coupling and dynamics. *J. Phys. Chem. B* **109,** 11512–11519 (2005).
18. Ortiz, W., Roitberg, A. E. & Krause, J. L. Molecular dynamics of poly(benzylphenyl ether) dendrimers: Effects of backfolding on Forster energy-transfer rates. *J. Phys. Chem. B* **108,** 8218–8225 (2004).
19. Melinger, J. S. *et al.* Optical and photophysical properties of light-harvesting phenylacetylene monodendrons based on unsymmetrical branching. *J. Am. Chem. Soc.* **124,** 12002–12012 (2002).
20. Atas, E., Peng, Z. H. & Kleiman, V. D. Energy transfer in unsymmetrical phenylene ethynylene dendrimers. *J. Phys. Chem. B* **109,** 13553–13560 (2005).
21. Tretiak, S., Saxena, A., Martin, R. L. & Bishop, A. R. Interchain electronic excitations in poly(phenylenevinylene) (PPV) aggregates. *J. Phys. Chem. B* **104,** 7029–7037 (2000).
22. Chernyak, V., Volkov, S. N. & Mukamel, S. Exciton coherence and electron energy loss spectroscopy of conjugated molecules. *Phys. Rev. Lett.* **86,** 995–998 (2001).
23. Chernyak, V., Volkov, S. N. & Mukamel, S. Electronic structure-factor, density matrices, and electron energy loss spectroscopy of conjugated oligomers. *J. Phys. Chem. A* **105,** 1988–2004 (2001).
24. Bonchev, D. & Mekenyan, O. G. (eds) in *Graph Theoretical Approaches to Chemical Reactivity* (Kluwer Academic, Boston, 1994).
25. Piryatinski, A., Stepanov, M., Tretiak, S. & Chernyak, V. Semiclassical scattering on conical intersections. *Phys. Rev. Lett.* **95,** 223001 (2005).
26. Dreuw, A. & Head-Gordon, M. Single-reference ab initio methods for the calculation of excited states of large molecules. *Chem. Rev.* **105,** 4009–4037 (2005).
27. Tretiak, S., Igumenshchev, K. & Chernyak, V. Exciton sizes of conducting polymers predicted by time-dependent density functional theory. *Phys. Rev. B* **71,** 33201 (2005).
28. Anand, S. *et al.* Optical excitations in carbon architectures based on dodecadehydrotribenzo[18]annulene. *J. Phys. Chem. A* **110,** 1305–1318 (2006).
29. Mukamel, S., Tretiak, S., Wagersreiter, T. & Chernyak, V. Electronic coherence and collective optical excitations of conjugated molecules. *Science* **277,** 781–787 (1997).
30. Tretiak, S., Saxena, A., Martin, R. L. & Bishop, A. R. Conformational dynamics of photoexcited conjugated molecules. *Phys. Rev. Lett.* **89,** 097402 (2002).
31. Tretiak, S. & Mukamel, S. Density matrix analysis and simulation of electronic excitations in conjugated and aggregated molecules. *Chem. Rev.* **102,** 3171–3212 (2002).
32. Jang, S. J. & Silbey, R. J. Theory of single molecule line shapes of multichromophoric macromolecules. *J. Chem. Phys.* **118,** 9312–9323 (2003).
33. Coulson, C. A. & Longuet-Higgins, H. C. The electronic structure of conjugated systems. I. General theory. *Proc. R. Soc. Lond. A* **191,** 39–60 (1947).
34. Altmann, S. L. π–σ; electronic states in molecules. I. The Hückel approximation. *Proc. R. Soc. Lond. A* **210,** 327–343 (1952).
35. Frisch, M. J. *et al. Gaussian 03* (Rev. C.02) (Gaussian, Wallingford, Connecticut, 2003).

Acknowledgements

V.Y.C. acknowledges the support through the start-up funds from WSU. The research at LANL is supported by the Center for Integrated Nanotechnology (CINT), the Center for Nonlinear Studies (CNLS) and the OBES program of the US Department of Energy. This support is gratefully acknowledged.
Correspondence and requests for materials should be addressed to S.T. or V.Y.C.

Competing financial interests

The authors declare that they have no competing financial interests.